Journal of Alloys and Compounds 524 (2012) 26–31

Contents lists available at SciVerse ScienceDirect

Journal of Alloys and Compounds

journal homepage: www.elsevier.com/locate/jallcom

High resolution X-ray diffraction study of InAs layers grown with and without bismuth flow on GaAs substrates by metalorganic vapor phase epitaxy

T. Mzoughi, H. Fitouri, I. Moussa, A. Rebey*, B. El Jani

Université de Monastir, Unité de Recherche sur les Hétéro-Epitaxies et Applications, Faculté des Sciences de Monastir, 5000 Monastir, Tunisia

ARTICLE INFO

Article history:
Received 23 September 2011
Received in revised form 22 January 2012
Accepted 31 January 2012
Available online 11 February 2012

Keywords:
Metalorganic vapor phase epitaxy
InAs
High resolution X-ray diffraction

PACS:
81.05.Ea
81.15.Gh
61.05.Cp

ABSTRACT

InAs layers were grown with and without bismuth flow by atmospheric pressure metalorganic vapor phase epitaxy on exactly oriented, 2° and 10° misoriented (1 0 0) GaAs substrates. Structural analysis was carried out using high resolution X-ray diffraction. Without bismuth flow, only InAs layers grown on 10° misoriented substrates exhibit a mosaic structure. Layers grown on exactly oriented and 2° misoriented substrates show large full widths at half maxima of their diffraction rocking curves. Growing InAs under bismuth flow leads to the reduction of this full width indicating a clear improvement of their structural quality. Particularly for samples grown on 10° misoriented substrates, a complete disappearance of the mosaic structure was obtained. The crystalline quality improvement is attributed to the contribution of Bi nanodots in relieving strain.

© 2012 Elsevier B.V. All rights reserved.

1. Introduction

The epitaxial growth of InAs layers on GaAs substrates is of particular interest due to their application in several electronic devices specially in infrared detectors and lasers [1–3]. However, InAs on GaAs is highly lattice-mismatched system (~7%) leading to a high dislocation density at the heteroepitaxial interface. To overcome such problems, several technical methods were suggested. A two step method using InAs prelayer grown under In rich environment [4], or a graded buffer layer (InGaAs, InAlAs, GaInAlAs) [5,6], or a Te covered GaAs surface [7], have showed a clear improvement of the physical properties of active InAs layer. Substrate orientation and growth parameters were found to change the energy of surface reconstructions, the kinetics of adsorption, migration and desorption of adatoms [8–12]. Indeed, growth at lower temperatures or under low V/III ratio eliminated the multiple tilting of InAs crystal planes giving rise to InAs films aligned with their substrates [13]. Many studies using misoriented GaAs substrates were also carried out to evaluate the microstructure and development of defects in epitaxial InAs films [14–16]. On the other hand, the use of surfactants in such mismatched systems as Te [17] and Sb [18] and Bi [19] provides a layer by layer growth mode, increases the critical layer thickness and ameliorates the surface quality. Bismuth solubility in III–V compounds is very low and reaches approximately 0.025% in InAs [20]. Due to its large size, bismuth segregates on the surface and does not incorporate easily in InAs matrix [19,21]. When growing InAs quantum dots by metalorganic vapor phase epitaxy (MOVPE) on (1 0 0) GaAs substrates, Bi was used as surfactant [22], but there is still no report indicating Bi effect on crystalline quality of InAs epilayers.

In this paper, the structural characterization of InAs layers grown by atmospheric pressure MOVPE on exactly oriented, 2° and 10° misoriented (1 0 0) GaAs substrates with and without Bi flow is reported. The effect of Bi on the structural quality and on the surface morphology of InAs layers is discussed.

2. Experimental methods

The epitaxial InAs layers were deposited simultaneously on different (1 0 0) GaAs substrates by atmospheric pressure MOVPE. These substrates are (1 0 0) exactly oriented and misoriented by 2° and 10° towards [1 1 1]A direction. Trimethylindium (TMI) and pure arsine (AsH_3) were used as source materials. The carrier gas was Pd-diffused H_2. The substrate temperature was measured by a thermocouple inserted into the graphite succeptor. In order to remove the native surface oxide layer the substrates were first ramped in a mixture flow of H_2 and AsH_3 at 700 °C for 10 min. After, the temperature was decreased till 450 °C and stabilized to grow InAs layers at a fixed V/III ratio of 18. Under these conditions another set of InAs layers were grown on GaAs substrates under trimethylbismuth (TMBi) flow ($TMBi/AsH_3 = 0.005$). High resolution X-ray diffraction (HRXRD), analysis were performed with a diffractometer using $\lambda_{CuK\alpha 1} = 1.54056$ Å radiation from a Discover D8 (40 KV, 55 mA) high

* Corresponding author. Tel.: +216 73 500 274; fax: +216 73 500 278.
E-mail addresses: hedi.fitouri@fsm.rnu.tn (H. Fitouri), ahmed.rebey@fsm.rnu.tn (A. Rebey).

0925-8388/$ – see front matter © 2012 Elsevier B.V. All rights reserved.
doi:10.1016/j.jallcom.2012.01.160

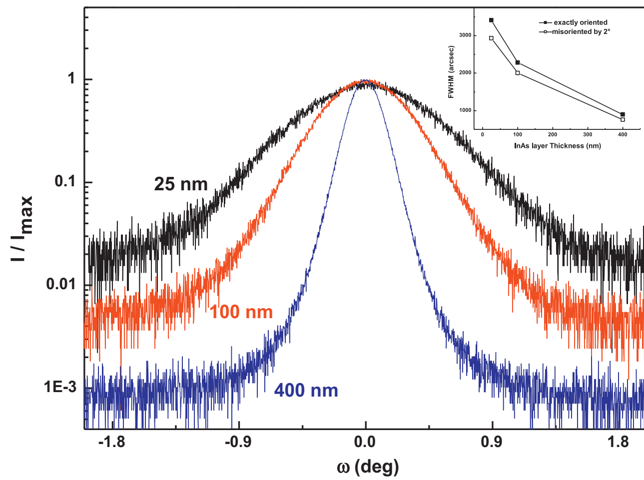

Fig. 1. (0 0 4) normalized RC of InAs layers with different thicknesses grown on exactly oriented (1 0 0) GaAs substrates. The inset shows the FWHM variation versus thickness.

power X-ray generator. Surface analysis was carried out using a scanning electron microscope (SEM).

3. Results and discussion

In order to study the crystalline quality of InAs layers grown on different GaAs substrates, we have performed (0 0 4) HRXRD analysis of samples having different thicknesses. Fig. 1 shows typical diffraction rocking curves (RC) of InAs layers grown on exactly oriented GaAs substrates without TMBi flow. The intensity is plotted in a logarithmic scale to show the behavior around the half width. This figure indicates that the breadth of these peaks decreases with increasing InAs thickness. The full width at half maximum (FWHM) of the X-ray diffraction RCs scans are shown in the insert as a function of InAs thicknesses grown on exactly oriented and 2° misoriented (1 0 0) GaAs substrates. The FWHM decreases with increase in film thickness. The reduction of FWHM can be caused by several phenomena, as well as defect and dislocation, grain size broadening, or strain fluctuation. The average dislocation density and the diameter of the particle size can be determined by the Eqs. (1) and (2) respectively [23]:

$$D = \frac{FWHM^2}{(4b)^2} \quad (1)$$

$$G = \frac{\lambda}{\cos(\theta_b)\,FWHM} \quad (2)$$

Where b is the Burgers vector, θ_b is Bragg angle and λ is the radiation wavelength. The dislocation density and grain size as a function of the layer thickness are shown in Fig. 2. We note that the particle sizes of the InAs layers increase, but the dislocation density decreases with increasing film thickness. The thick layer is formed of high particle size, that is to say, characterized by a better crystalline quality compared to other layers. SEM is used to estimate the dislocation density. Fig. 3 shows a SEM image of thick InAs layer (400 nm). Pits are observed at the surfaces which reveal the distribution of dislocations in the epitaxial layer. The density of pits calculated from the SEM images of three InAs layers is also presented in Fig. 2. However, the one-to-one correspondence between pits and dislocations provides a convenient method for estimating dislocation densities in these samples. Basing on the theoretical

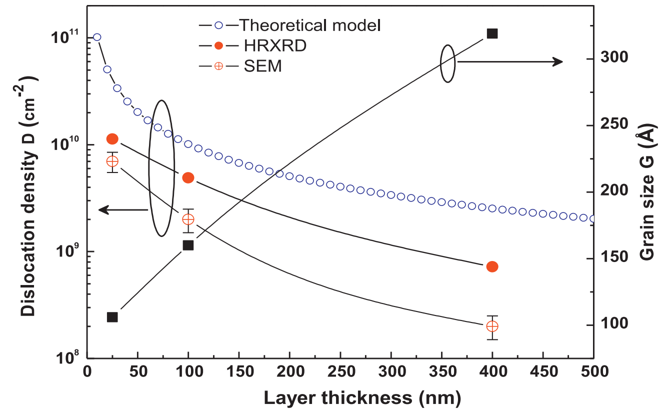

Fig. 2. Dislocation density (left axis) and grain size (right axis) as a function of epilayer thickness for InAs layers grown on exactly oriented (1 0 0) GaAs substrates.

model describing in ref. [24], the dislocation density is given by the following equation:

$$D = \frac{f\cos(\phi)}{16hb(1-\nu)}\ln\left(\frac{1}{4f}\right) \quad (3)$$

Where ν is the layer Poisson ratio, b is the length of the Burgers vector, f is the lattice mismatch, h is the layer thickness and ϕ is the angle between the threading segments and the interface. The theoretical dislocation density was then compared with the values obtained from the HRXRD and the SEM techniques. A notable difference was remarked. This discrepancy had several reasons. Indeed, the pits density appeared on the surface seem to be underestimated compared to the true dislocation density revealed in the entire layer by transmission electron microscopy. Another possible effect may stem from the depth dependence of the dislocation density. For each thickness, layers grown on 2° misoriented substrates exhibit FWHMs slightly lower than those grown on exactly oriented ones. This small decrease may be attributed to the presence of surface steps acting as a lattice distortion corrector. In order to analyze the thickness effect on the layer relaxation a qualitative calculation of (0 0 4) diffracted intensity of InAs for two thicknesses (25 nm and 400 nm) is calculated by using X-ray dynamical theory. In Fig. 4, we report the results of this calculation for strained and fully relaxed states of InAs layer. For comparison, the experimental data for these

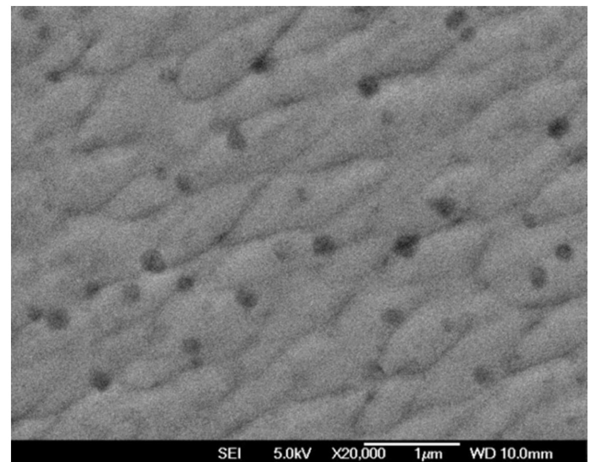

Fig. 3. SEM image of 400 nm InAs layer grown on exactly oriented (1 0 0) GaAs substrate.

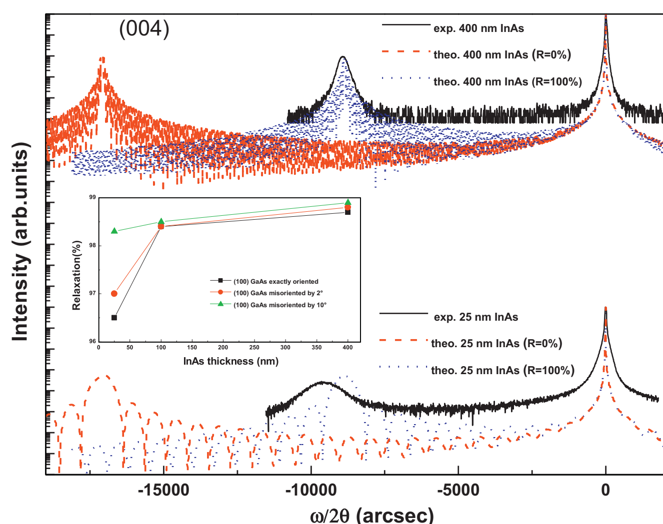

Fig. 4. Measured and calculated high resolution X-ray diffraction (0 0 4)$\omega/2\theta$ curves of InAs/GaAs layers for two thicknesses (25 nm, and 400 nm). The dashed and dotted line corresponds to the theoretical X-ray diffraction for strained (R = 0%) and fully relaxed (R = 100%) states of InAs layer respectively. The inset shows the relaxation coefficient as a function of InAs thickness for different misoriented GaAs substrates.

two thicknesses are added in the same figure. It should be noted that by increasing thickness the layer is more relaxed. Indeed, to quantify this observation we have measured a symmetric (0 0 4) and asymmetric (1 1 5) reflexions of $\omega/2\theta$ diffraction curves. We deduced the lattice parameters in growth direction ($a_\perp$) and in the plane ($a_{//}$), then the relaxation coefficient as defined by:

$$R = \frac{a_{//} - a_s}{a_0 - a_s}$$

Where a_0 and a_s are the lattice parameters of bulk InAs and GaAs substrate respectively. The inset of Fig. 4 representing the relaxation coefficient as a function of layer thickness confirms the qualitative observation. It is clear that thinnest InAs layers are more strained than thickest ones.

On the other hand, for 25 nm thick, the lattice parameter decreases with increasing substrate misorientation angle. This may be the effect of surface steps in decreasing compressive strain. In a previous work [25], we have shown that the thinnest InAs layer (25 nm), grown on exactly oriented GaAs substrate, presents a tilt amplitude of about 1.61° with respect to [0 0 1] direction. Due to the significant difference between InAs and GaAs thermal expansion coefficients, residual strain takes place during cooling of InAs layer [26] and becomes more remarkable on thinner layers. To explain the origin of this tilt amplitude, we have performed a (0 0 4) RCs for several positions in the thinnest InAs layer surface to determine the radius of curvature. This layer is slightly curved compared to its substrate indicating that InAs layer is under compression. Concerning the thickest InAs layer (400 nm) grown on 10° misoriented GaAs substrate, we present in Fig. 5 (0 0 4) diffraction RCs for three azimuthal angles φ. For φ = 160° and φ = 6°, two diffraction peaks are resolved. When azimuthal angle becomes equal to 74°, recorded maxima are overlapped giving rise to only one peak. The presence of these peaks is ensured by different RCs recorded in the open detector geometry corresponding to several ($h\,k\,l$) Bragg reflections. Fig. 6 shows typical diffraction profiles of (0 0 2), (0 0 4), (1 1 7) and (2 4 6) Bragg reflections recorded at an azimuthal angle of 160°. The breadth of diffraction profiles increases with increasing diffraction order showing also two resolved peaks. Such finding indicates that InAs layer is a mosaic of crystal blocks diffracting

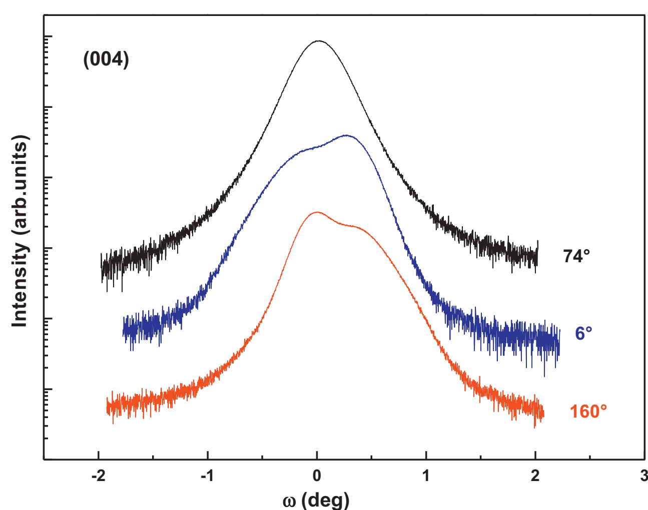

Fig. 5. High resolution X-ray diffraction (0 0 4) experimental RC of 400 nm InAs layer, grown on 10° misoriented GaAs substrate, for three azimuthal angles φ.

independently of each other. The farthest splitting ($\Delta\theta$) measured between these peaks in both Figs. 5 and 6 is of about 0.6°. This splitting corresponds to the maximum tilt between InAs grains in the film. Indeed, Khandekar et al. [13] have measured higher peak splitting values reaching 7° when growing InAs on GaAs substrates under higher V/III ratio (~80) and higher growth temperature (700 °C). The formation of mosaic structure is the reduction in strain energy resulting from the clustering of dislocations in interface and in the grain boundaries. The dislocation reorganization into mosaic structure takes place under internal or external stress during plastic relaxation. However, for a similar thickness (400 nm), all RCs of InAs layers grown on exactly oriented and 2° misoriented GaAs substrates, present a single peak and layers are well aligned with their substrates. In disoriented substrates, surface steps number increases with increasing misorientation angle. Unlike 10°, in exactly oriented and 2° misoriented substrates, the elastic strain exerted by the lower number of surface steps is less pronounced, and induces a small lattice constant change over the width of the step, acting as a lattice distortion corrector [27]. So higher misorientation angles of GaAs substrates, and lattice mismatch promote

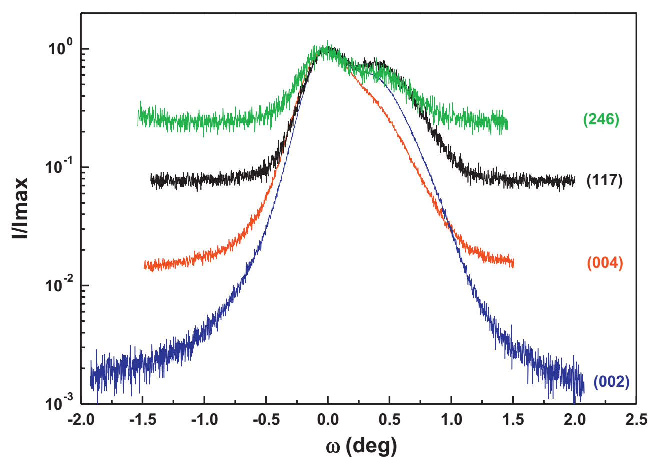

Fig. 6. Normalized RC profiles of the (0 0 2), (0 0 4), (1 1 7) and (2 4 6) Bragg reflections of 400 nm InAs layer grown on GaAs substrate misoriented by 10°.

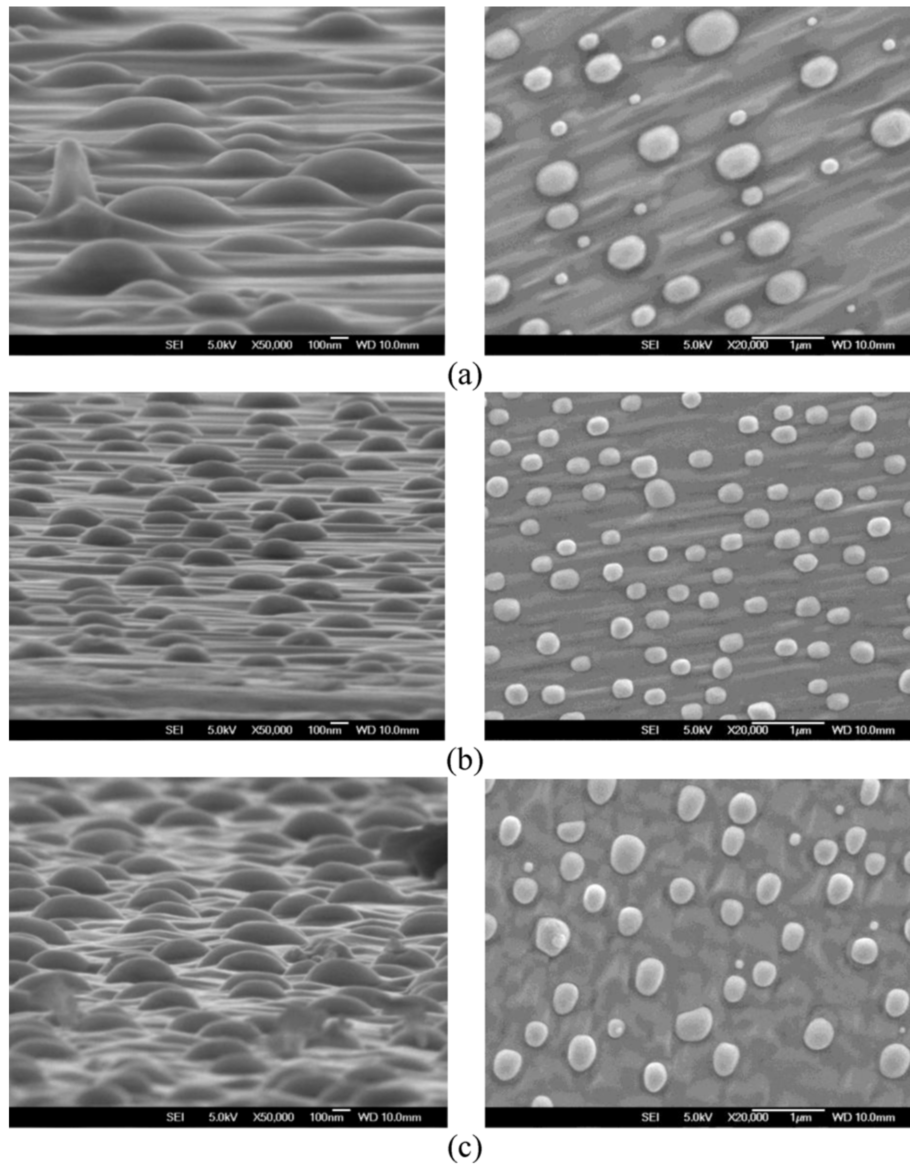

Fig. 7. SEM images of InAs layers grown on different misoriented GaAs substrates under TMBi flow (a) exactly oriented, (b) 2° and (c) 10° misoriented GaAs substrates.

dislocations spread from the interface to all over the layer surface. This may explains the appearance of mosaic structure only on 10° misoriented substrates.

To analyze Bi effect on the physical properties of InAs layers, we have preserved the same growth conditions. Thus, InAs layers were grown under TMBi flow on exactly oriented and misoriented GaAs substrates. Adding bismuth during growth should have a detectable effect on the crystal quality and surface morphology of InAs layers. In order to investigate these effects, we first compared the surface morphology of InAs layers grown with and without TMBi flow. AFM images of InAs samples grown on different misoriented (1 0 0) GaAs substrates without TMBi flow showing flat surfaces are presented elsewhere [25]. Fig. 7 shows the surface morphologies of InAs layers grown on exactly oriented and misoriented GaAs substrates under TMBi flow. Small inclusions of Bi nanodots randomly distributed and penetrating through the layer can be clearly seen. SEM images of these three samples show that density and size of Bi nanodots depend on substrates misorientation angle. We report in Fig. 8, the variation of Bi nanodots density and their average width

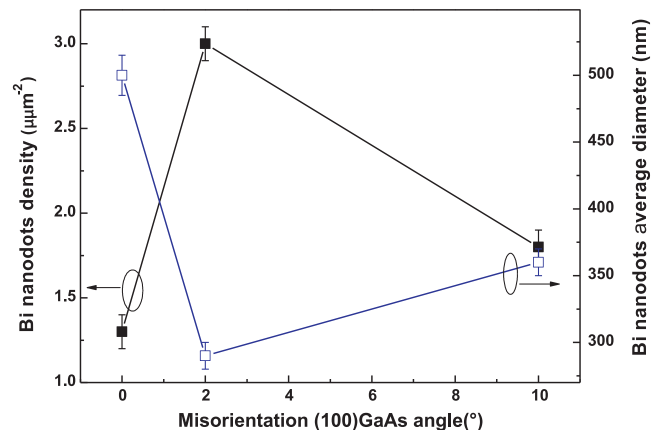

Fig. 8. Misoriented GaAs substrates dependence of Bi nanodots density (indicated by closed squares) and the average width of the Bi nanodots (indicated by open squares).

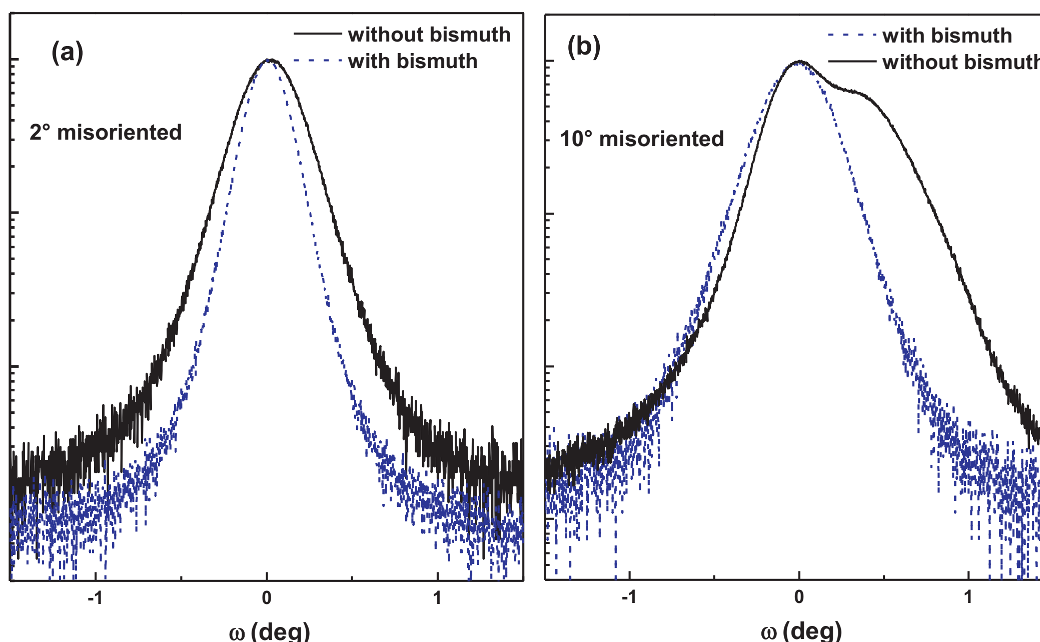

Fig. 9. High resolution X-ray diffraction (0 0 4) experimental RC of InAs layers grown with TMBi flow (lower curves) and without TMBi flow (upper curves) on 2° and 10° misoriented GaAs substrates.

as a function of (1 0 0) GaAs substrates misorientation angle. Theses average values were deduced from an AFM and SEM statistical analyses. Indeed, the highest density of Bi nanodots with a smaller size is observed on InAs layers grown on 2° misoriented substrate. However, this density decreases when using 10° misoriented substrate, but the size becomes bigger. For InAs layer grown on exactly oriented substrate, Bi nanodots are the biggest with the smallest density. The second point of comparison concerns the structural quality of InAs layers grown with and without TMBi flow. Fig. 9 shows (0 0 4) RCs of the thickest InAs layers (400 nm) grown on misoriented GaAs substrates at 450 °C with and without TMBi flow. We remark that TMBi induces a significant decrease in the FWHM of diffraction RCs. The measured value of the FWHM of the InAs layer grown on 2° misoriented substrate without TMBi flow is 1100 arcs and decreases to 760 arcs for that grown with TMBi. In addition, both peaks recorded in InAs layer grown on 10° misoriented substrate were disappeared giving rise to a single peak. However, a very small decrease (10 arcsec) of the FWHM was found in InAs layers grown on exactly oriented substrate. It seems that bismuth improves the crystal quality of layers grown only on misoriented substrates by reducing dislocation density and eliminating mosaic structure.

To find out an eventual secondary effect of Bi on the structural properties of InAs layers grown on different GaAs substrates, we have measured their tilt amplitude with respect to the substrate. RCs scans were achieved for various azimuthal angles φ. We report in Fig. 10, the diffraction angles variation of the substrate (ω_S) and the InAs layer (ω_L) for different azimuthal angles φ. All the measured amplitudes of the cosine variation of ω_S and ω_L, show a well aligned InAs layer–GaAs substrate. This tilt free is due to the In rich environment created by low growth temperature (450 °C) and low V/III ratio (18) [25]. The improvement of the crystalline quality observed in InAs layers grown on 2° misoriented substrates and the vanishing of the mosaic structure in InAs layers grown on 10° misoriented substrate is attributed to the presence of Bi nanodots inlayed in InAs film. In fact, on exactly oriented surface, Bi atoms segregation leads to bigger size (~500 nm) nanodots formation. However, step edges in misoriented surfaces facilitate Bi atoms nucleation and reduce the segregation phenomenon. That is why, for misoriented substrates, SEM images show a higher Bi nanodots density with a smaller size (~300 nm). These nanodots, improve the structural quality of InAs layers by relieving a part of the important strain. This may explain the reduction of the FWHM when using 2° misoriented substrates and the vanishing of mosaic structure. Since Bi nanodots density in InAs layers grown on exactly oriented substrate is low, a minor effect on the strain relieve is expected. Finally, the presence of Bi nanodots, in InAs layers grown on misoriented substrates, undoubtedly improves their crystal quality without bringing any tilt to the epilayers.

The electrical properties of InAs layers grown on exactly oriented and misoriented (1 0 0) GaAs substrates with and without TMBi flow were determined by room temperature Hall Effect measurements using the Van der Pauw configuration. Our results of this investigation are established that all the samples exhibit n-type conduction. We remark that TMBi induces a significant improvement in the measured electron mobility. Indeed, the measured electron mobility of the thick InAs layer grown on 2° misoriented substrate without TMBi flow is about 410 $cm^2 V^{-1} s^{-1}$and increases to 2400 $cm^2 V^{-1} s^{-1}$ for that grown with TMBi. For the layers grown on exactly oriented and 10° misoriented substrates with TMBi flow, the measured electron mobility is also about 2400 $cm^2 V^{-1} s^{-1}$ which is the twice of the value for InAs grown on the same substrates without TMBi. The improvement of the measured electron mobility in the layers grown under TMBi flow is attributed to the existence of Bi nanodots. Since scattering in the surface and GaAs interface dominate the conductivity mechanism, the presence of Bi metallic nanodots increases the carrier mobility.

Finally, basing on these investigations we have deduced that bismuth incorporation in InAs matrix is very low (of about 0.4%). Such characterizations by photoluminescence and photoreflectance in IR range can give more qualifications of the Bi nonodots effect on the layers optical properties.

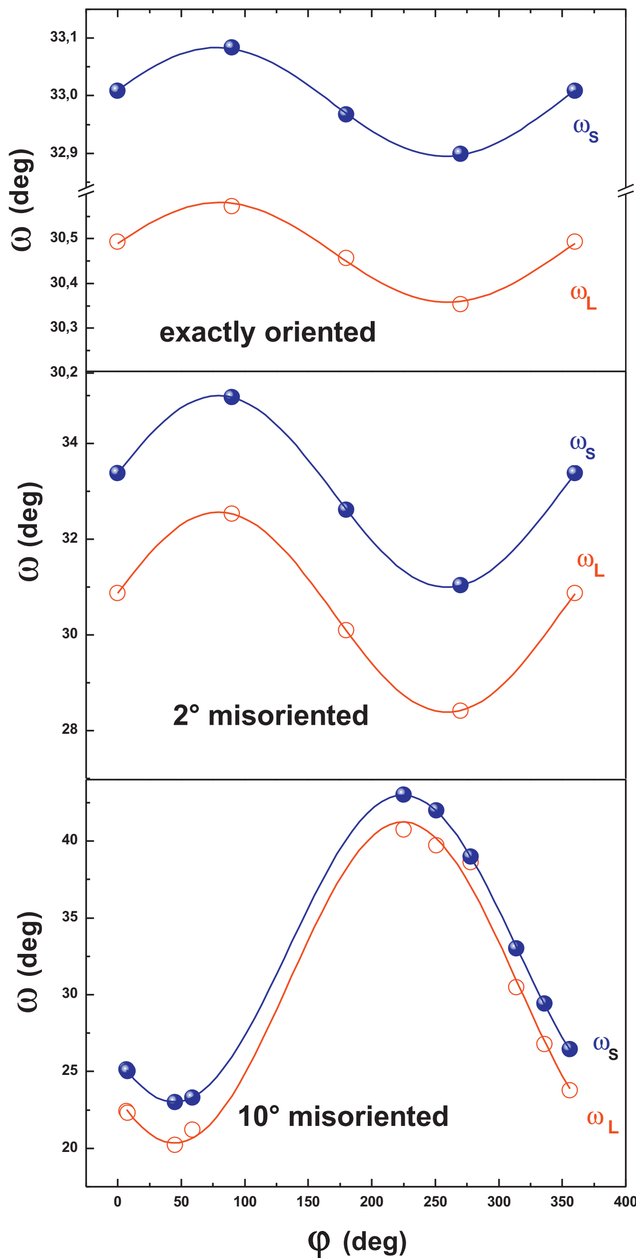

Fig. 10. Diffraction angles variation of GaAs substrate ω_S and InAs layer ω_L versus azimuthal angle φ for exactly oriented, 2° and 10° misoriented GaAs substrates.

4. Conclusion

The effect of TMBi flow on the structural properties of InAs layers grown on exactly oriented, 2° and 10° misoriented GaAs substrates was investigated. X-ray diffraction analysis of layers grown on 2° and 10° misoriented substrates show a decrease in the FWHM of the diffraction RC and a vanishing of mosaic structure respectively. The crystalline quality improvement is attributed to Bi nanodots participating in relieving strain. For layers grown on exactly oriented substrate, no significant effect on their crystal quality was found. This was explained by the lower density of Bi nanodots. Hall Effect measurements show a clear increase of the electron mobility for the layers grown with TMBi flow.

Acknowledgement

The research was supported by the DGRST.

References

[1] S.-W. Lee, K. Hirakawa, Y. Shimada, Appl. Phys. Lett. 75 (1999) 1428.
[2] R.A. Rupani, S. Ghosh, X. Su, P. Bhattacharya, Microelectron J. 39 (2008) 307.
[3] G. Yusa, H. Sakaki, Appl. Phys. Lett. 70 (1997) 345.
[4] H. Chen, L.C. Cai, C.L. Bao, J.H. Li, Q. Huang, J.M. Zhou, Cryst. Growth J. 208 (2000) 795.
[5] A. Bosacchi, A.C. De Riccardis, P. Frigeri, S. Franchi, C. Ferrari, S. Gennari, L. Lazzarini, L. Nasi, G. Salviati, A.V. Drigo, F. Romanato, J. Cryst. Growth 175/176 (1997) 1009.
[6] W.E. Hoke, T.D. Kennedy, A. Torabi, C.S. Whelan, P.F. Marsh, R.E. Leoni, C. Xu, K.C. Hsieh, J. Cryst. Growth 251 (2003) 827.
[7] N. Grandjean, J. Massies, V.H. Etgens, Phys. Rev. Lett. 69 (1992) 796.
[8] Q. Xue, T. Ogino, H. Kiyama, Y. Hasegawa, T. Sakurai, J. Cryst. Growth 175/176 (1997) 174.
[9] Z.L. Miao, S.J. Chua, S. Tripathy, C.K. Chia, Y.H. Chye, P. Chen, J. Cryst. Growth 268 (2004) 18.
[10] S.K. Haywood, R.W. Martin, N.J. Mason, P.J. Walker, J. Cryst. Growth 97 (1989) 489.
[11] H. Naoi, D.M. Shaw, Y. Naoi, S. Sakai, G.J. Collins, J. Cryst. Growth 250 (2003) 290.
[12] A.A. Khandekar, G. Suryanarayanan, S.E. Babcock, T.F. Kuech, J. Cryst. Growth 275 (2005) 1067.
[13] A.A. Khandekar, G. Suryanarayanan, S.E. Babcock, T.F. Kuech, J. Cryst. Growth 292 (2006) 40.
[14] R.S. Goldman, K.L. Kavanagh, H.H. Wieder, S.N. Ehrlich, R.M. Feenstra, J. Appl. Phys. 83 (1998) 5137.
[15] C.-I. Liao, K.-F. Yarn, C.-L. Lin, Y.-H. Yang, Jpn. J. Appl. Phys. 41 (2002) 1247.
[16] P. Maigne, A.P. Roth, Semicond. Sci. Technol. 7 (1992) 1.
[17] W.N. Rodrigues, V.H. Etgens, M. Sauvage-Simkin, G. Rossi, F. Sirotti, R. Pinchaux, F. Rochet, Solid State Commun. 95 (1995) 873.
[18] R. Timm, H. Eisele, A. Lenz, T.Y. Kim, F. Streicher, K. Potschke, U.W. Pohl, D. Bimberg, M. Dahne, Physica E 32 (2006) 25.
[19] G. Feng, K. Oe, M. Yoshimoto, J. Cryst. Growth 301–302 (2007) 121.
[20] K.Y. Ma, Z.M. Fang, R.M. Cohen, G.B. Stringfellow, J. Appl. Phys. 70 (1991) 3940.
[21] K.T. Huang, C.T. Chiu, R.M. Cohen, G.B. Stringfellow, J. Cryst. Growth 134 (1993) 29.
[22] B.N. Zvonkov, I.A. Karpovich, N.V. Baidus, D.O. Filatov, S.V. Morozov, Y.Y. Gushina, Nanotechnology 11 (2000) 221.
[23] L. Tapfer, J.R. Martinez, K. Ploog, Semicond. Sci. Technol. 4 (1989) 617.
[24] J.E. Ayers, J. Appl. Phys. 78 (1995) 3724.
[25] H. Ben Naceur, I. Moussa, O. Tottereau, A. Rebey, B. El Jani, Physica E 41 (2009) 1779.
[26] H. Yuan, S.J. Chua, Z. Miao, J. Dong, Y. Wang, J. Cryst. Growth 273 (2004) 63.
[27] J.E. Ayers, S.K. Ghandhi, L.J. Schowalter, J. Cryst. Growth 113 (1991) 430.